

The Role of Gluons in Dilepton Production from the Quark-Gluon Plasma

Ziwei Lin and C. M. Ko

Cyclotron Institute and Physics Department, Texas A&M University, College Station, TX 77843

Abstract

We study dilepton production from gluon-induced processes, $gq \rightarrow q\gamma^*$, $g\bar{q} \rightarrow \bar{q}\gamma^*$, and $gg \rightarrow q\bar{q}\gamma^*$, in a thermally equilibrated but chemically under-saturated partonic matter that is expected to be created in the initial stage of ultrarelativistic heavy ion collisions. Regulating the divergence in these processes by the thermal quark mass, we find that gluon-induced processes are more important than the leading-order $q\bar{q}$ annihilation process as a result of the larger number of gluons than quarks in the partonic matter. The dependence of the thermal dilepton yield from the partonic stage of heavy ion collisions on the initial conditions for the partonic matter is also studied. We further discuss the feasibility of observing thermal dileptons from the quark-gluon plasma in heavy ion experiments.

1 Introduction

One suggested signature for verifying the formation of a quark-gluon plasma (QGP) in heavy ion collisions at the Relativistic Heavy Ion Collider (RHIC) is the thermal dileptons it produces. Many studies have thus been carried out to calculate the expected dilepton yield from the QGP. In earlier works, contributions from the leading-order (LO) $q\bar{q}$ annihilation process [1] and processes up to $\mathcal{O}(\alpha_s)$ [2, 3] have been evaluated by assuming that the QGP is in both thermal and chemical equilibrium. Although thermal equilibrium can be reached in the partonic matter created in heavy ion collisions at RHIC energies, chemical equilibrium is, however, unlikely to be established [4, 5]. Furthermore, since the partonic matter is dominated by gluons, the thermal dilepton yield from LO $q\bar{q}$ annihilation processes is thus much smaller than that from the initial Drell-Yan process and final charm decays [6].

The dominance of gluons in the initial partonic matter gives rise to the interesting possibility that dilepton production from gluon-induced processes may become more important than LO $q\bar{q}$ annihilation processes, even though they are suppressed by powers of α_s . In this paper, we shall study thermal dilepton production from gluon-induced processes, i.e., the Compton processes ($gq \rightarrow q\gamma^*$ and $g\bar{q} \rightarrow \bar{q}\gamma^*$) and processes with two initial-state gluons ($gg \rightarrow q\bar{q}\gamma^*$). In particular, we shall consider these processes only at leading order in α_s , i.e., at $\mathcal{O}(\alpha_s)$ and $\mathcal{O}(\alpha_s^2)$ for the Compton and two-gluon processes, respectively.

This paper is organized as follows. In Section 2, we introduce the thermal quark mass in a non-equilibrium partonic matter at finite temperature, which will be used

in Section 3 to regulate the divergent dilepton production cross sections for gluon-induced reactions. Thermal dilepton rates are then calculated in Section 4 for an under-saturated partonic matter in thermal equilibrium. In Section 5, we estimate the total thermal dilepton yield in heavy ion collisions at RHIC energies and study its dependence on the initial conditions for the partonic matter. We then compare it with the Drell-Yan yield to see if thermal dileptons from the QGP can be observed in experiments. Finally, a summary and discussions are given in Section 6.

2 The Thermal Quark Mass

For a partonic matter in thermal equilibrium at temperature T but out of chemical equilibrium, the parton distributions can be written in the Jüttner form,

$$f_i = \frac{\lambda_i}{e^{\beta u \cdot p} \pm \lambda_i}, \quad (1)$$

where i denotes different parton species, $\beta = 1/T$, and u is the four velocity of the local comoving frame. In the limit of small fugacities ($\lambda_i \ll 1$), the parton distribution functions reduce to the Boltzmann form,

$$f_i \simeq \lambda_i e^{-\beta u \cdot p}. \quad (2)$$

Assuming that the partonic matter is both baryon and flavor symmetric with N_f quark flavors, i.e., $\lambda_{q_i} = \lambda_{\bar{q}_i} = \lambda_q$ ($i = 1, N_f$), then two fugacity parameters, λ_g and λ_q , are needed to specify the degree of chemical equilibrium.

Since chemical equilibration of the partonic matter created in heavy ion collisions at RHIC is likely to be slow, we shall use the Boltzmann distribution of Eq.(2) in the following calculations unless specified otherwise. In this case, parton densities in the local comoving frame are directly related to fugacities as

$$n_g = \lambda_g \frac{d_g T^3}{\pi^2}, \quad n_q + n_{\bar{q}} = \lambda_q \frac{(d_q + d_{\bar{q}}) N_f T^3}{\pi^2}, \quad (3)$$

if partons are assumed to be massless. In the above, d_i is the degeneracy factor of parton i , i.e., $d_g = 2(N_c^2 - 1)$ and $d_q = d_{\bar{q}} = 2N_c$.

The thermal quark mass, denoted as μ , is given by

$$\mu^2 = 4\pi\alpha_s \frac{N_c^2 - 1}{2N_c} \int \frac{d^3p}{(2\pi)^3} \frac{1}{p} (f_g + f_q), \quad (4)$$

where $\alpha_s = g^2/(4\pi)$ is the QCD strong coupling. For a QGP in chemical equilibrium, this gives a thermal quark mass $\mu^2 = g^2 T^2/6$, when the exact parton distributions of Eq.(1) are used. For an under-saturated partonic system described approximately by Eq.(2), the thermal quark mass becomes

$$\mu^2 = \frac{2g^2 T^2}{3\pi^2} (\lambda_g + \lambda_q). \quad (5)$$

3 Dilepton Production Cross Sections

Processes that are leading-order in α_s for dilepton production from different initial parton states are $q\bar{q}$ annihilation ($q\bar{q} \rightarrow \gamma^*$), Compton processes ($gq \rightarrow q\gamma^*$ and $g\bar{q} \rightarrow \bar{q}\gamma^*$), two-gluon fusion ($gg \rightarrow q\bar{q}\gamma^*$), and two-quark ($qq \rightarrow qq\gamma^*$) and two-antiquark bremsstrahlung ($\bar{q}\bar{q} \rightarrow \bar{q}\bar{q}\gamma^*$). They are of order $\mathcal{O}(1)$, $\mathcal{O}(\alpha_s)$, $\mathcal{O}(\alpha_s^2)$, $\mathcal{O}(\alpha_s^2)$ and $\mathcal{O}(\alpha_s^2)$, respectively, in the strong coupling constant. In the following, we neglect two-quark and two-antiquark bremsstrahlung as they do not involve gluons in the initial state and are also suppressed by α_s^2 relative to the LO $q\bar{q}$ process. In Fig.1, we show the diagrams being considered in our study.

Cross sections for dilepton production from partons can be generally written as

$$\frac{d\hat{\sigma}_{ij}}{dM^2} = \frac{4\pi\alpha^2}{9M^2\hat{s}} W_{ij}. \quad (6)$$

In the above, indices i and j specify initial-state partons, $\hat{s} = (p_i + p_j)^2$, and α is the fine structure constant. The quantity W_{ij} is related to the square of the transition amplitude. For the leading-order $q\bar{q}$ annihilation process, it is simply

$$W_{q\bar{q}} = e_q^2 \delta(1 - \xi), \quad (7)$$

with $\xi = M^2/\hat{s}$.

For Compton processes, the squared matrix element, after averaging over initial and summing over final spins and colors, is given by

$$\overline{|M_{gq \rightarrow q\gamma^*}|^2} = \overline{|M_{g\bar{q} \rightarrow \bar{q}\gamma^*}|^2} = \frac{(4\pi)^2 \alpha \alpha_s e_q^2}{3} \left[-\frac{\hat{t}}{\hat{s}} - \frac{\hat{s}}{\hat{t}} + \frac{2M^2(\hat{s} + \hat{t} - M^2)}{\hat{s}\hat{t}} \right]. \quad (8)$$

The total cross section, given by $\hat{\sigma} = \int dt \overline{|M|^2} / (16\pi\hat{s}^2)$, is divergent. For the Drell-Yan process this divergence can be absorbed into the definition of parton structure functions in a hadron after calculating divergent terms in a certain regularization scheme and including virtual corrections. Studies of dilepton production from the quark-gluon plasma based on the finite temperature QCD [2, 3] show that this divergence of order $\mathcal{O}(\alpha_s)$ can be consistently removed, as in thermal photon production [7]. Because of our limited understanding of dilepton production from a non-equilibrium partonic matter in the finite temperature QCD, we take a simple approach in this study by using the thermal quark mass as the screening mass to regulate all divergences in thermal dilepton production. We thus replace $1/\hat{t}$ with $1/(\hat{t} - \mu^2)$, and Eq.(8) then becomes

$$\overline{|M_{gq \rightarrow q\gamma^*}|^2} \simeq \frac{(4\pi)^2 \alpha \alpha_s e_q^2}{3} \left[-\frac{\hat{t}}{\hat{s}} - \frac{\hat{s}}{\hat{t} - \mu^2} + \frac{2M^2(\hat{s} + \hat{t} - M^2)}{\hat{s}(\hat{t} - \mu^2)} \right]. \quad (9)$$

After integrating over \hat{t} we obtain

$$W_{gq} = W_{g\bar{q}} = \frac{\alpha_s e_q^2}{4\pi} c_0(\xi), \quad (10)$$

where

$$c_0(\xi) = \frac{1 + 2\xi - 3\xi^2}{2} + \left[1 - 2\xi \left(1 - \xi + \frac{\mu^2}{M^2} \xi \right) \right] \ln \left(1 + \frac{M^2}{\mu^2} \frac{1 - \xi}{\xi} \right). \quad (11)$$

There are no studies on dilepton production from two-gluon fusion processes, $gg \rightarrow q\bar{q}\gamma^*$, at finite temperature. However, processes involving heavy quarks in the final state such as $gg \rightarrow Q\bar{Q}\gamma^*$ have been studied in determining the K-factor in Drell-Yan processes in the limit of $M^2 \gg m_Q^2$ [8, 9]. In this study, we thus only consider dileptons with an invariant mass $M \geq 2$ GeV. Since $M^2 \gg \mu^2$ unless the temperature is extremely high, we can replace the heavy quark mass m_Q in Ref. [8, 9] with the thermal quark mass μ and obtain

$$W_{gg} = e_q^2 \left(\frac{1}{2} \right)^2 \left(\frac{\alpha_s}{4\pi} \right)^2 \left[c_1(\xi) \ln^2 \frac{M^2}{\mu^2} + c_2(\xi) \ln \frac{M^2}{\mu^2} + c_3(\xi) \right]. \quad (12)$$

In the above, the functions $c_1(\xi)$, $c_2(\xi)$ and $c_3(\xi)$ can be obtained from Ref.[8], where the calculation was carried out in the $\overline{\text{MS}}$ scheme.

4 Thermal Dilepton Rates

For a partonic matter in thermal equilibrium at a temperature T but out of chemical equilibrium, the thermal dilepton rates are given by

$$\frac{dR_{ij}}{dM} = S_{ij} \sum \int \frac{d^3 p_1}{(2\pi)^3} f_i(p_1) \frac{d^3 p_2}{(2\pi)^3} f_j(p_2) v_{\text{rel}} \frac{d\hat{\sigma}_{ij}}{dM}(M, \sqrt{\hat{s}}), \quad (13)$$

with $v_{\text{rel}} = (p_1 \cdot p_2)/(p_1 p_2)$, $S_{gg} = 1/2$ accounting for identical gluons in the initial state, and $S_{ij} = 1$ otherwise. The summation is over parton spin and color indices.

The integrals in the above equation can be evaluated using the rapidity and transverse momentum variables,

$$\begin{aligned} \hat{s} &= M_0^2, \quad P_0^\mu = (M_{\perp 0} \cosh Y_0, P_{\perp 0} \cos \Phi_0, P_{\perp 0} \sin \Phi_0, M_{\perp 0} \sinh Y_0), \\ p_1^\mu &= p_{\perp 1} (\cosh y_1, \cos \phi_1, \sin \phi_1, \sinh y_1), \end{aligned} \quad (14)$$

where $M_{\perp 0} = \sqrt{M_0^2 + P_{\perp 0}^2}$. Inserting $\int d^4 P_0 \delta^4(P_0 - p_1 - p_2)$ into Eq.(13), then the delta function can be used to remove the $\int d^3 p_2$ and $\int dp_{\perp 1}$ integrals. After integrating over Φ_0 and redefining $y_1 - Y_0$ and $\phi_1 - \Phi_0$ as y_1 and ϕ_1 , we obtain

$$\begin{aligned} \frac{dR_{ij}}{dM} &= \frac{d_i d_j \lambda_i \lambda_j S_{ij}}{4(2\pi)^5} \int dM_0 dY_0 dM_{\perp 0} d\phi_1 dy_1 \\ &\times \frac{M_{\perp 0} M_0^5 e^{-M_{\perp 0} \cosh(Y_0 - \eta)/T}}{(M_{\perp 0} \cosh y_1 - P_{\perp 0} \cos \phi_1)^2} \frac{d\hat{\sigma}_{ij}}{dM}(M, M_0). \end{aligned} \quad (15)$$

Carrying out the integrals over Y_0 and ϕ_1 and then those over y_1 and $M_{\perp 0}$, we obtain

$$\frac{dR_{ij}}{dM} = \frac{d_i d_j \lambda_i \lambda_j S_{ij}}{(2\pi)^4} \int_M dM_0 M_0^4 T K_1(M_0/T) \frac{d\hat{\sigma}_{ij}}{dM}(M, M_0). \quad (16)$$

Summing over quark flavors, we finally get

$$\begin{aligned}
\frac{dR_{q\bar{q}}}{dM} &= \alpha^2 \lambda_q^2 \frac{F_q}{\pi^3} M^2 T K_1(M/T), \\
\frac{dR_{gq+g\bar{q}}}{dM} &= \alpha^2 \alpha_s \lambda_g \lambda_q \frac{8F_q}{3\pi^4} \frac{T}{M} \int_M dM_0 M_0^2 K_1(M_0/T) c_0(\xi), \\
\frac{dR_{gg}}{dM} &= \alpha^2 \alpha_s^2 \lambda_g^2 \frac{F_q}{9\pi^5} \frac{T}{M} \int_M dM_0 M_0^2 K_1(M_0/T) \\
&\quad \times \left[c_1(\xi) \ln^2 \frac{M^2}{\mu^2} + c_2(\xi) \ln \frac{M^2}{\mu^2} + c_3(\xi) \right], \tag{17}
\end{aligned}$$

with

$$F_q = \sum_{i=1}^{N_f} e_{qi}^2 = \frac{5}{9} \text{ for } N_f = 2. \tag{18}$$

For the strong coupling constant, we use the following LO value with three quark flavors

$$\alpha_s = \frac{4\pi}{9 \ln \frac{M^2}{\Lambda^2}}, \tag{19}$$

with $\Lambda = 200$ MeV and the normalization scale chosen to be the dilepton mass M .

In the limit $M^2 \gg \mu^2$, the thermal dilepton rates depend on the coupling constants and fugacities as

$$\begin{aligned}
\frac{dR_{q\bar{q}}}{dM} &\propto \alpha^2 \lambda_q^2, \\
\frac{dR_{gq+g\bar{q}}}{dM} &\propto \alpha^2 \alpha_s \lambda_g \lambda_q \ln \frac{1}{\lambda_g + \lambda_q}, \\
\frac{dR_{gg}}{dM} &\propto \alpha^2 \alpha_s^2 \lambda_g^2 \ln^2 \frac{1}{\lambda_g + \lambda_q}. \tag{20}
\end{aligned}$$

In Fig. 2, we show the thermal dilepton rates from a quark-gluon plasma in full thermal and chemical equilibrium at $T = 570$ MeV. It is seen that for dileptons with mass above 2 GeV LO $q\bar{q}$ annihilation processes give the dominant contribution, while Compton processes give a small contribution, and that from two-gluon processes is even smaller. These results are not unexpected as Compton and two-gluon processes are suppressed by α_s and α_s^2 , respectively.

The situation is, however, very different if partons are not in chemical equilibrium. As an example, we show in Fig. 3 the thermal dileptons rates for $T = 570$ MeV, $\lambda_g = 0.060$ and $\lambda_q = 0.0072$. The reason for choosing these values will be given in the next Section. In this case, Compton processes produce more thermal dileptons than the LO $q\bar{q}$ annihilation, and even two-gluon fusion processes give a comparable contribution to lower-mass dileptons. As a result, the total thermal dilepton yield is significantly enhanced by gluonic processes.

The appreciable difference between results shown in Fig. 3 and Fig. 2 can be qualitatively understood from the scaling behavior given in Eq.(20). Because of the quadratic dependence on parton fugacities, gluonic processes become dominant over the $q\bar{q}$ processes when gluons greatly outnumber quarks ($\lambda_g/\lambda_q \gg 1$). Even if λ_g/λ_q is fixed but $\lambda_g \rightarrow 0$ in an under-saturated partonic matter, both $R_{gq+g\bar{q}}/R_{q\bar{q}}$ and $R_{gg}/R_{q\bar{q}}$ become logarithmic divergent, indicating that gluonic processes become more important than $q\bar{q}$ annihilation when the parton system is further away from chemical equilibrium.

To illustrate this quantitatively, we show in Fig. 4 the full-equilibrium results in Fig. 2 multiplied by the quadratic fugacity factors. In this case Compton processes are already as important as the $q\bar{q}$ annihilation. Further increase of the gluonic contributions when going from Fig. 4 to Fig. 3 is due to the logarithmic terms in Eq.(20), which come from the thermal quark mass in the regulated partonic cross sections given by Eqs.(10-12).

We also see in Figs. 2-4 that LO $q\bar{q}$ annihilation processes are most effective in producing high invariant-mass dileptons because all incoming energy can be used. In contrast, there are one or two partons in the final state in Compton and two-gluon fusion processes to carry away part of the incoming energy. To produce high mass dileptons from these processes thus requires more energetic partons, which are less available. Therefore, the three curves in Fig. 3 corresponding to the above three processes exhibit increasingly larger slopes.

5 Thermal Dilepton Yields at RHIC

In this Section, we estimate the thermal dilepton yield in central Au+Au collisions at RHIC by integrating the thermal dilepton rate over the space-time four volume that is determined from schematic models. Also, we will study the feasibility of observing the thermal dilepton signal in experiments by comparing it with the Drell-Yan background.

Starting from Eq.(15) and using $d^4x = \tau d\tau d\eta d^2x_\perp$, we first integrate over η instead of Y_0 and then over ϕ_1 , y_1 and $M_{\perp 0}$ as in previous section. This gives

$$\frac{dN_{ij}}{dM} = \int dY_0 d\tau \tau d^2x_\perp \frac{d_i d_j \lambda_i \lambda_j S_{ij}}{(2\pi)^4} \int_M dM_0 M_0^4 T K_1(M_0/T) \frac{d\hat{\sigma}_{ij}}{dM}(M, M_0), \quad (21)$$

which then leads to

$$\frac{dN_{ij}}{dM^2 dY_0} = \int_{\tau_0}^{\tau_f} d\tau \tau d^2x_\perp \frac{dR_{ij}}{dM^2}(\tau). \quad (22)$$

In the above, τ_0 is the initial proper time when the parton system first reaches thermal equilibrium, and τ_f is the final proper time when the temperature drops to T_c (chosen to be 200 MeV) for the phase transition to a hadronic matter. The rates dR_{ij}/dM^2 depend on τ implicitly through the time evolution of the variables λ_i , T and μ .

We note that while the pair rapidity Y_0 of the two partons in the initial state is equal to the pair rapidity Y of the dilepton in LO $q\bar{q}$ annihilation processes, they are

different in gluon-induced processes. However, in the case that the Bjorken scaling is assumed for the expansion of the partonic matter, the dependence of the thermal dilepton yield on Y and Y_0 must have the following functional form:

$$\frac{dN}{dM^2 dY dY_0} = F(Y - Y_0, M), \quad (23)$$

as a result of boost invariance of the integrand on the right-hand side of Eq.(13). This thus gives

$$\frac{dN}{dM^2 dY} = \frac{dN}{dM^2 dY_0}. \quad (24)$$

The same argument applies to η , and it is easy to verify that

$$\frac{dN}{dM^2 d\eta} = \frac{dN}{dM^2 dY_0}. \quad (25)$$

5.1 Time evolution of parton fugacities and temperature

First, we need to specify the time evolution of partons in the quark-gluon phase created in heavy ion collisions at RHIC. Earlier studies [6] based on kinetic equations including $2 \leftrightarrow 3$ gluonic processes have shown that thermal equilibrium is achieved first, and both gluon and quark fugacities increase as the system evolves. However, since the quark-gluon plasma has only a finite lifetime of several fm/ c , chemical equilibrium is unlikely to be established, and parton fugacities thus remain well below the value of unity. To take into account such effects, we follow Fig. 25 of Ref.[6] by simply assuming that the parton fugacities increase linearly with the proper time,

$$\lambda_i = \lambda_{i,0} \left(\frac{\tau}{\tau_0} \right). \quad (26)$$

In an ideal hydrodynamic description, the temperature of the partonic matter decreases as $T \propto 1/\tau^{1/3}$, which then leads to a decrease of the rapidity density of transverse energy as $dE_T/dy \propto \tau T^4 \propto 1/\tau^{1/3}$. In the parton cascade model, the time evolution of the rapidity density of transverse energy depends sensitively on the magnitude of parton cross sections and densities [10]. Since we do not expect the rapidity density of transverse energy to change more than 25% during the partonic stage of RHIC heavy ion collisions [10, 11], we assume for simplicity that dE_T/dy , given by

$$\frac{dE_T}{dy} = \frac{dN}{dy} \langle p_\perp \rangle \propto \left(\sum_i d_i \lambda_{i,0} \right) \tau T^3 T \propto (\tau T^2)^2, \quad (27)$$

is a constant. This then leads to the time evolution of temperature as

$$T = T_0 \left(\frac{\tau_0}{\tau} \right)^{1/2}. \quad (28)$$

In the above, we have used

$$\frac{dN}{dy} = \tau_0 \pi R_A^2 \sum_i n_i \quad (29)$$

at central rapidity at τ_0 and $R_A \simeq 1.12A^{1/3}$ fm. Also, we neglect the transverse expansion throughout this study.

In Fig. 5 the time evolutions of the fugacities and temperature given in Eqs.(26) and (28) are shown. We see that the temperature decreases faster than that given by the scenario of entropy conservation, i.e., $T \propto 1/\tau^{1/3}$. This is expected because parton production increases the entropy.

5.2 The default scenario

As in Ref. [6], where the parton equilibration is studied using kinetic equations, we assume that at the proper time $\tau_0=0.7$ fm/ c , thermal equilibrium is established at a temperature $T_0 = 570$ MeV. We also take the same gluon and quark densities at τ_0 as in Ref. [6], and obtain the following values for the initial parton fugacities [12]:

$$\lambda_{g,0} = 0.060 \text{ and } \lambda_{q,0} = 0.0072. \quad (30)$$

With these values, we find that quarks and antiquarks make about 15% of the partons and the thermal quark mass is about 75 MeV if the strong coupling constant is evaluated at the normalization scale of 2 GeV. Subsequent expansion of the partonic matter is assumed to follow the Bjorken scaling.

We have evaluated the thermal dilepton yield using Eq.(22), and the results are shown in Fig. 6. Also shown is the expected Drell-Yan yield from primary hard collisions with a K-factor of 1.7, obtained from fitting the E772 data, to take into account higher-order contributions. As in thermal dilepton rates shown in Fig.3, we find that more dilepton are produced from Compton processes than from LO $q\bar{q}$ annihilation processes, and the two-gluon fusion is less important. Despite the enhancement from gluonic processes, the total thermal dilepton yield is still a factor of 30 or more (depending on the dilepton mass) below the Drell-Yan yield. It thus seems quite difficult to observe the thermal dileptons in heavy ion collisions at RHIC.

5.3 An upper limit

The small thermal dilepton yield discussed in the above default scenario is mainly due to the small number of quarks and antiquarks compared to that of gluons assumed in the initial conditions for partons. While we have used the ratio of initial quarks to gluons that is consistent with minijet calculations based on perturbative QCD together with initial and final state radiations, it is possible that additional soft partons may be produced. Also, there may be already some chemical equilibration before the thermal stage starts at τ_0 . Both could then lead to initial quark fugacities that are larger than the estimate from minijet calculations.

To obtain an upper limit for the thermal dilepton yield, we assume that quarks and antiquarks are in relative chemical equilibrium with gluons at the initial time τ_0 , i.e., $\lambda_q = \lambda_{\bar{q}}$, although both are still out of full chemical equilibrium. Requiring the same value of total dE_T/dy at central rapidity as before, we obtain from Eq.(27) and using the same τ_0 and T_0 the following upper limit (UL) for the initial parton fugacities:

$$\lambda_{g,0}^{UL} = \lambda_{q,0}^{UL} = \frac{d_g \lambda_{g,0} + (d_q + d_{\bar{q}}) N_f \lambda_{q,0}}{d_g + (d_q + d_{\bar{q}}) N_f} \simeq 0.028. \quad (31)$$

This gives a ratio of 3/5 for the sum of quarks and antiquarks to the total number of partons, similar to that in an ideal gas of gluons and quarks with $N_f = 2$.

Using the same time evolution as given by Eqs.(26) and (28), we have evaluated the thermal dilepton yield with the above initial parton condition, and the results are shown in Fig.7. Because of increased number of quarks and antiquarks, the contribution from LO $q\bar{q}$ processes is increased by a factor of about 16, while gluonic processes become less important in comparison. As a result, the total thermal dilepton yield is about a factor of six higher than that in the default scenario. Depending on the dilepton mass, this is still about a factor of 5 or more below the Drell-Yan yield.

5.4 Dependence on initial parton conditions

Thermal dilepton yields are sensitive to the initial conditions, such as τ_0 and T_0 in our model. For example, the contribution from $q\bar{q}$ annihilation given in Eq.(17) depends on temperature as

$$\frac{dR_{q\bar{q}}}{dM} \propto T^{3/2} e^{-M/T}. \quad (32)$$

The thermal dilepton yields can be large if the partonic matter starts at a very high initial temperature T_0 . In the following, we study the dependence of the thermal dilepton yield on the parameters $\lambda_{g,0}$, $\lambda_{q,0}$, τ_0 and T_0 .

For a fully-equilibrated QGP at $T_0 = 570$ MeV with $N_f = 2$ and a starting proper time $\tau_0 = 0.7$ fm/c, the rapidity density of transverse energy is ¹

$$\frac{dE_T}{dy} = \tau_0 \pi R_A^2 \frac{\pi}{4} \left(\frac{8}{15} + \frac{7N_f}{20} \right) \pi^2 T_0^4 \sim 12,000 \text{ GeV} \quad (33)$$

at central rapidity. This is more than an order of magnitude larger than most model estimates of the final dE_T/dy .

In the default scenario, on the other hand, Eq.(29) with $\lambda_{g,0} = 0.060$, $\lambda_{q,0} = 0.0072$, $\tau_0 = 0.7$ fm/c and $T_0 = 570$ MeV gives at central rapidity

$$\frac{dE_T}{dy} = \frac{dN}{dy} \frac{3\pi T}{4} \sim 350 \text{ GeV}. \quad (34)$$

¹Bose-Einstein and Fermi-Dirac distributions are used.

Including additional E_T from subsequent string fragmentation gives a final $dE_T^F/dy \sim 900$ GeV at central rapidity, which is comparable with predictions from most event generators and cascade models for heavy ion collisions at RHIC energies.

We shall thus study the dependence of thermal dilepton yields on initial conditions that have the same value of initial dE_T/dy at central rapidity. According to Eq.(27), this is equivalent to taking initial conditions with the constraint

$$\left(\sum_i d_i \lambda_{i,0} \right) \tau_0 T_0^4 = \text{const.} \quad (35)$$

We have already studied the effect due to the increase of the quark fraction in the partonic matter. Here, we study the dependence on initial conditions with a fixed $\lambda_{g,0}/\lambda_{q,0}$, i.e., with same values of both $\lambda_{g,0}\tau_0 T_0^4$ and $\lambda_{q,0}\tau_0 T_0^4$.

Using the same time evolutions in Eqs.(26) and (28), LO $q\bar{q}$ annihilation processes give

$$\begin{aligned} \frac{dN_{q\bar{q}}}{dM^2 dY} &\simeq \frac{\pi R_A^2}{2M} \int_{\tau_0}^{\tau_f} d\tau \tau \frac{dR_{q\bar{q}}}{dM}(\tau) \propto \int_{\tau_0}^{\tau_f} d\tau \tau \lambda_q^2 T K_1\left(\frac{M}{T}\right) \\ &\propto \left(\lambda_{q,0}\tau_0 T_0^4\right)^2 \int_{\frac{M}{T_c}}^{\frac{M}{T_0}} dx x^6 K_1(x) \propto \int_{\frac{M}{T_0}}^{\infty} dx x^6 K_1(x). \end{aligned} \quad (36)$$

It is seen that the above contribution depends only on one dimensionless variable M/T_0 .

In Fig.8, we show the numerical results of the last integral in the above equation as a function of M/T_0 . As T_0 increases, the dilepton yield at a fixed mass M increases as the variable M/T_0 shifts to the left, and the yield saturates at the high temperature limit. The slow increase and final saturation with increasing initial temperature T_0 deviates from the naive expectation based on Eq.(32). This is due to the constraint on the total dE_T/dy in Eq.(35), which requires that as the initial temperature increases, the initial volume and/or the initial parton fugacities becomes smaller, thus making the total dilepton yield less sensitive to initial conditions. We also see that the yield of higher-mass dileptons depend more strongly on the initial temperature. However, in the dilepton mass range of 2 – 4 GeV, where the yield of thermal dileptons is closer to the Drell-Yan yield, the variable M/T_0 has a value between 3.5 to 7 when the default choice of $T_0 = 570$ MeV is used. Fig.8 thus shows that the maximum increase one obtains by increasing T_0 while keeping the same total dE_T/dy is only 15% at dilepton mass of 2 GeV and no more than a factor of 2 at dilepton mass of 4 GeV. Therefore, thermal dileptons are still well below the Drell-Yan yield even if we allow the maximum increase of the upper limit results in Fig. 7.

Same studies can be carried out for the Compton and two-gluon processes, but they involve more parameters other than the dimensionless variable M/T_0 due to the presence of the thermal quark mass μ . Relations similar to Eq.(36) can still be obtained except for the logarithmic factors shown in Eq.(20). Similar conclusions thus hold as long as the screening mass is not extremely small.

6 Discussions and Summary

We have studied thermal dilepton production in heavy ion collisions at RHIC energies. In particular, contributions from gluonic processes and the dependence on the initial parton conditions are investigated. We find that gluonic processes significantly enhance the thermal dilepton yield as there are more gluons than quarks in the partonic matter. However, the total thermal dilepton yield is still much lower than the Drell-Yan yield. Our results show that thermal dileptons can be observed only in a rather ideal case, when the initial energy density is higher than most current expectations, and parton chemical equilibration proceeds fast so that quarks are close to relative equilibrium with gluons.

There are many uncertainties in our study of thermal dilepton productions. First of all, the divergence of partonic cross sections has been simply regulated by the thermal quark mass μ . Since dilepton yields from Compton and two-gluon processes scale as $\log \mu$ and $\log^2 \mu$, respectively, the two sets of curves in Fig.9, corresponding to results using $\mu/2$ and 2μ as the screening mass, respectively, but with the default initial parton condition, show sizeable differences. A better treatment is to use finite-temperature QCD theory to calculate self-consistently the screening mass.

In this study, we have only considered dilepton production from the thermal stage, where partons are assumed to have reached thermal equilibrium. The contribution from the pre-thermal stage has not been included. Also, we have not considered chemical equilibration during the pre-thermal stage, which could change the initial conditions of the partonic matter such as the fugacities $\lambda_{g,0}$ and $\lambda_{q,0}$. With the parton cross sections for dilepton production obtained in Section 3, pre-thermal dilepton production can be calculated using either parameterized pre-thermal parton distributions or from a parton cascade code. With the latter, the whole history of parton thermal and chemical equilibration can be studied, so the separation of pre-thermal and thermal stages, which is rather crude, is unnecessary. In this way, the evolution of parton fugacities can be self-consistently determined, and all secondary dileptons from the partonic stage can be calculated.

In a previous study [13], we have carried out a calculation of secondary dileptons from LO $q\bar{q}$ annihilation processes within the parton cascade code ZPC [14], where initial parton fugacities were determined directly from the HIJING model [15]. Since the default HIJING model gives too few quarks and antiquarks, with the ratio of the sum of quarks and antiquarks to the total number of partons being only 4.5% (compared with the ratio of 15% in the default scenario of the present study based on minijet calculations using perturbative QCD), the thermal dilepton yield in Ref.[13] was lower than the default result in this study by a factor of 10.

We have also shown that with the constraint of Eq.(34) on the total initial dE_T/dy of the partonic matter, thermal dileptons are always significantly lower than those from the Drell-Yan process for any reasonable variations of the initial temperature, proper time, and fugacities. Only in a quark-rich partonic matter with an initial energy density much higher than the value we have used here, can thermal dileptons compete with those from the Drell-Yan process.

Acknowledgments: We thank B. Kampfer and S.M.H. Wong for helpful discussions. This work was supported in part by the National Science Foundation under Grant No. PHY-9870038, the Welch Foundation under Grant No. A-1358, and the Texas Advanced Research Project FY97-010366-068.

References

- [1] K. Kajantie, J. Kapusta, L. McLerran, A. Mekjian, Phys. Rev. D 34 (1986) 2746.
- [2] R. Baier, B. Pire, D. Schiff, Phys. Rev. D 38 (1988) 2814.
- [3] J. Cleymans, I. Dadić, Phys. Rev. D 47 (1993) 160.
- [4] E. Shuryak, Phys. Rev. Lett. 68 (1992) 3270.
- [5] T.S. Biro, E. van Doorn, B. Müller, M.H. Thoma, X.N. Wang, Phys. Rev. C 48 (1993) 1275.
- [6] X.-N. Wang, Phys. Rep. 280 (1997) 287.
- [7] R. Baier, M. Kirks, K. Redlich, D. Schiff, Phys. Rev. D 56(1997) 2548.
- [8] P.J. Rijken, W.L. van Neerven, Phys. Rev. D 52 (1995) 149.
- [9] R. Hamberg, W.L. van Neerven, T. Matsuura, Nucl. Phys. B 359 (1991) 343; W.L. van Neerven, E.B. Zijlstra, Nucl. Phys. B 382 (1992) 11.
- [10] M. Gyulassy, Y. Pang, B. Zhang, Nucl. Phys. A 626 (1997) 999.
- [11] B. Zhang, C.M. Ko, B.-A. Li, Z. Lin, preprint nucl-th/9907017.
- [12] The difference between our parton fugacity values ($\lambda_{g,0} = 0.060$, $\lambda_{q,0} = 0.0072$) and those in Ref.[6] ($\lambda_g^0 = 0.05$, $\lambda_q^0 = 0.008$) for the same parton number densities is due to the fact that we use the factorized Boltzmann distribution of Eq.(2) rather than the factorized Bose-Einstein and Fermi-Dirac distributions.
- [13] S. Bass *et al*, preprint nucl-th/9907090.
- [14] B. Zhang, Comp. Phys. Comm. 109 (1998) 193.
- [15] X.-N. Wang and M. Gyulassy, Phys. Rev. D 44 (1991) 3501; *ibid* 45 (1992) 844.

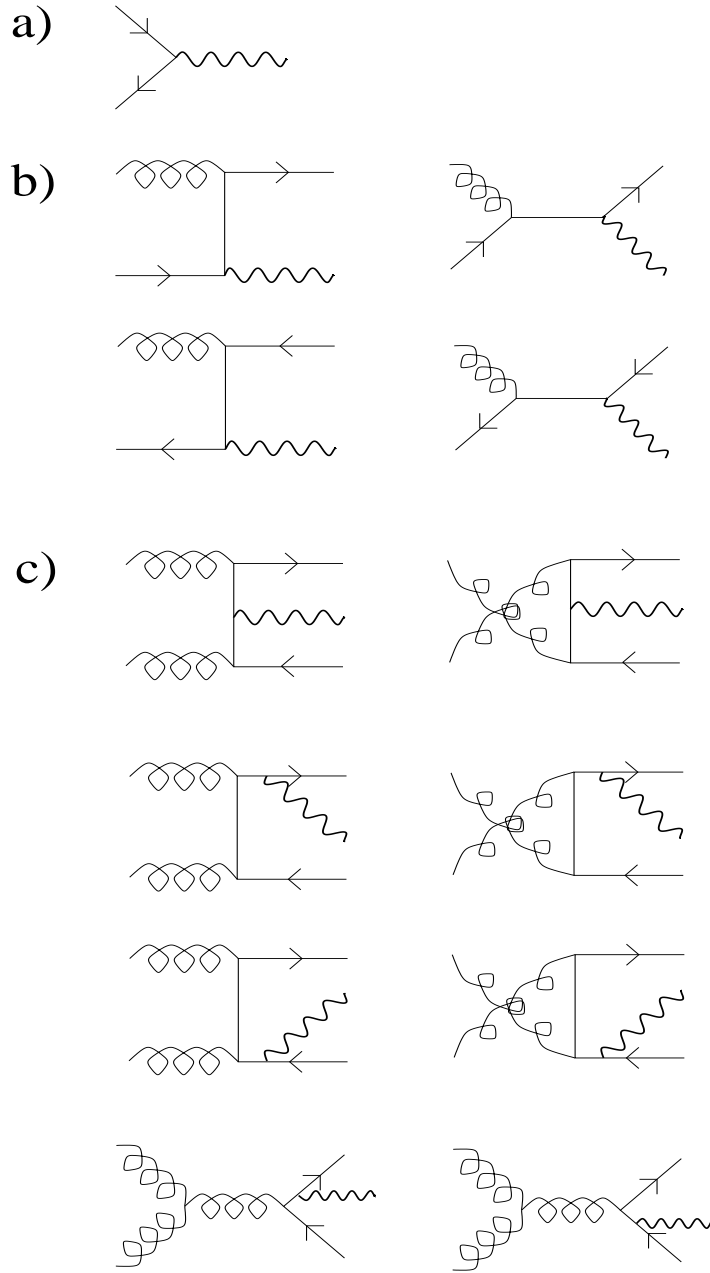


Figure 1: Diagrams for dilepton production: a) $q\bar{q}$ annihilation, b) Compton processes, and c) two-gluon fusion processes. Curly lines represent gluons, wavy lines represent virtual photons, and straight lines with arrows to the right (left) represent quarks (antiquarks).

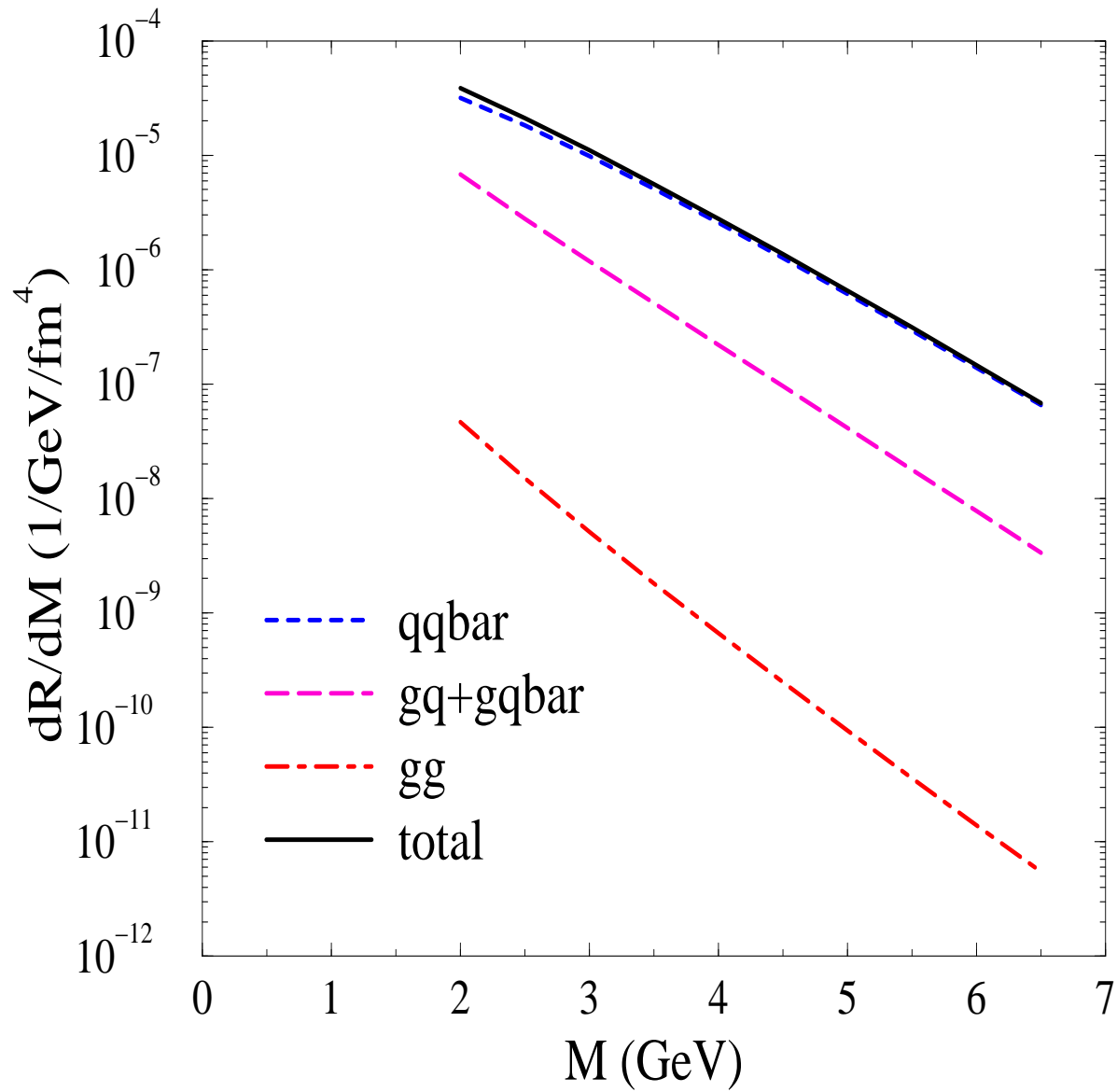


Figure 2: Thermal dilepton rates from a quark-gluon plasma in full thermal and chemical equilibrium at a temperature $T = 570$ MeV.

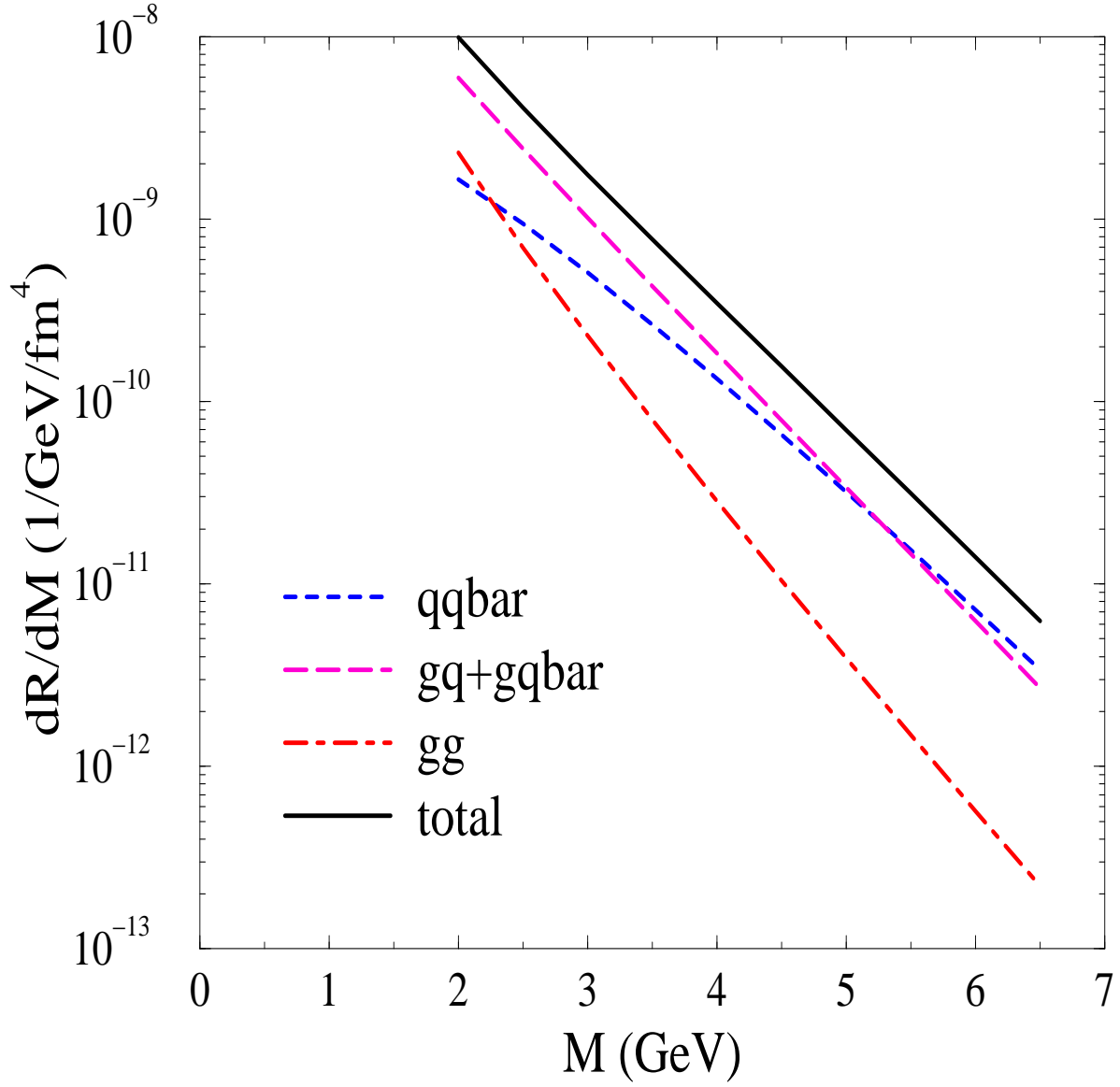


Figure 3: Thermal dilepton rates from a gluon-dominated, under-saturated quark-gluon plasma with $T = 570$ MeV, $\lambda_g = 0.060$ and $\lambda_q = 0.0072$.

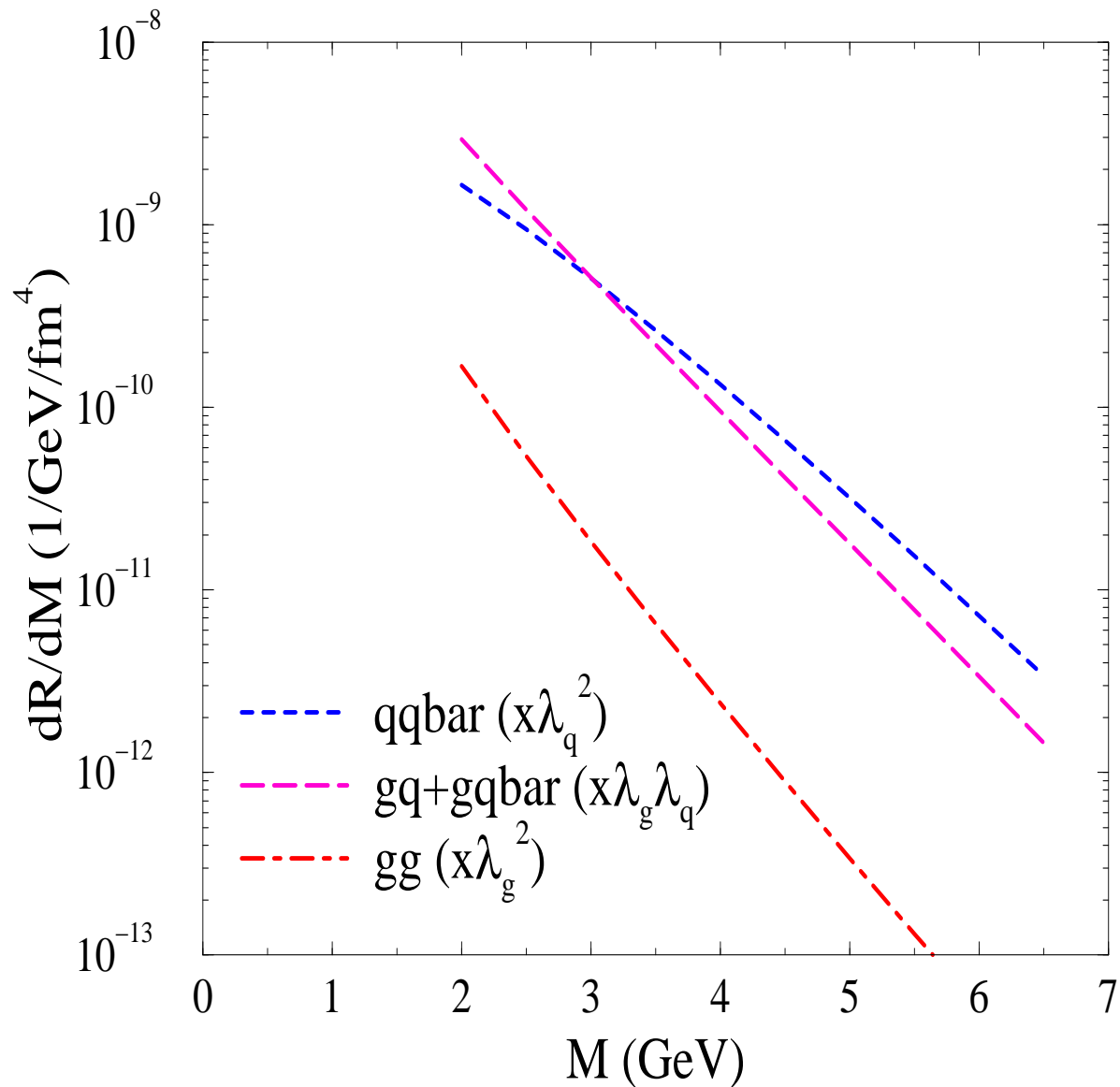


Figure 4: Thermal dilepton rates from a quark-gluon plasma in full thermal and chemical equilibrium at $T = 570$ MeV after being multiplied by the fugacity factors $\lambda_g = 0.060$ and $\lambda_q = 0.0072$.

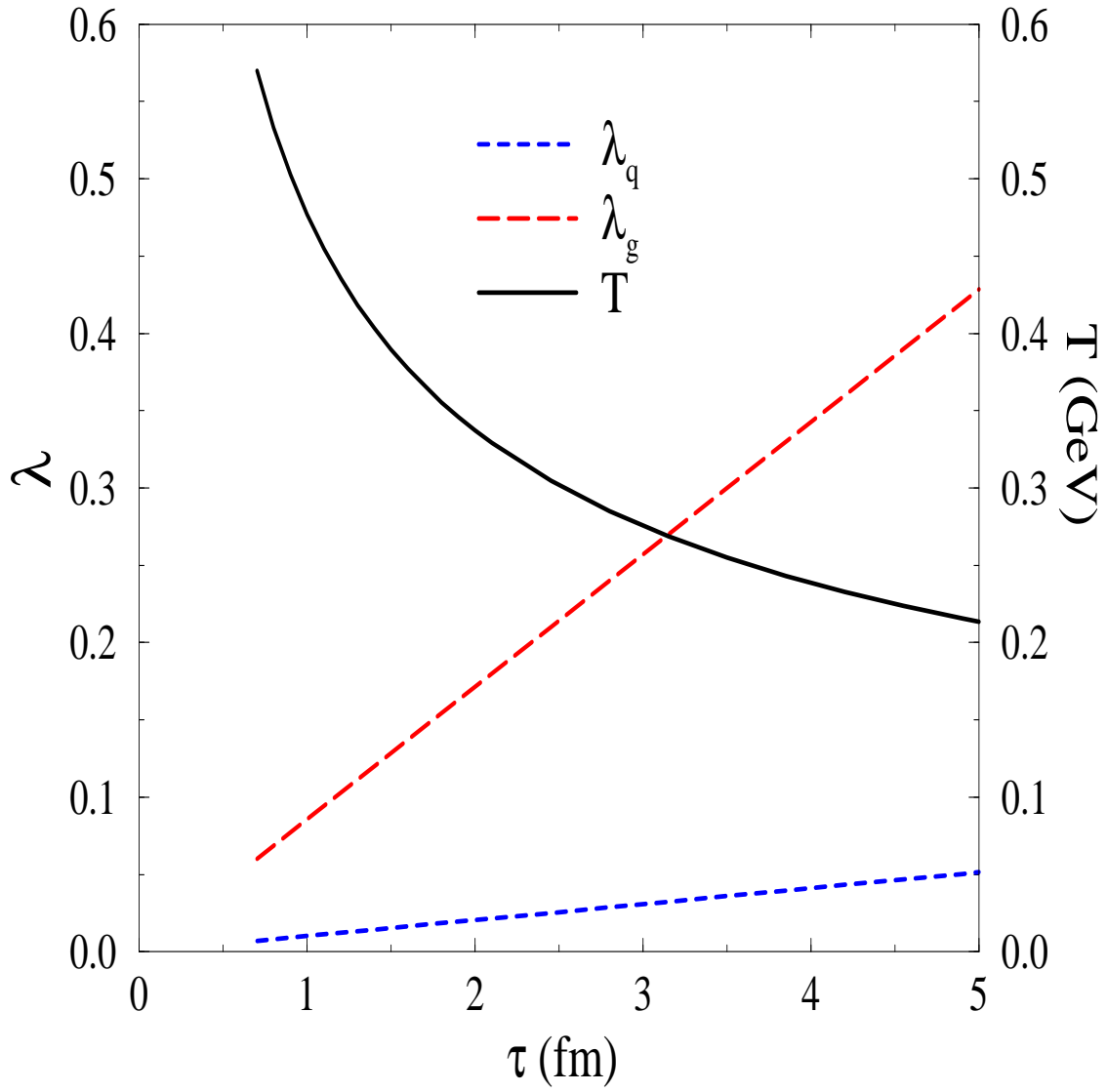


Figure 5: Time evolution of the parton fugacities and temperature.

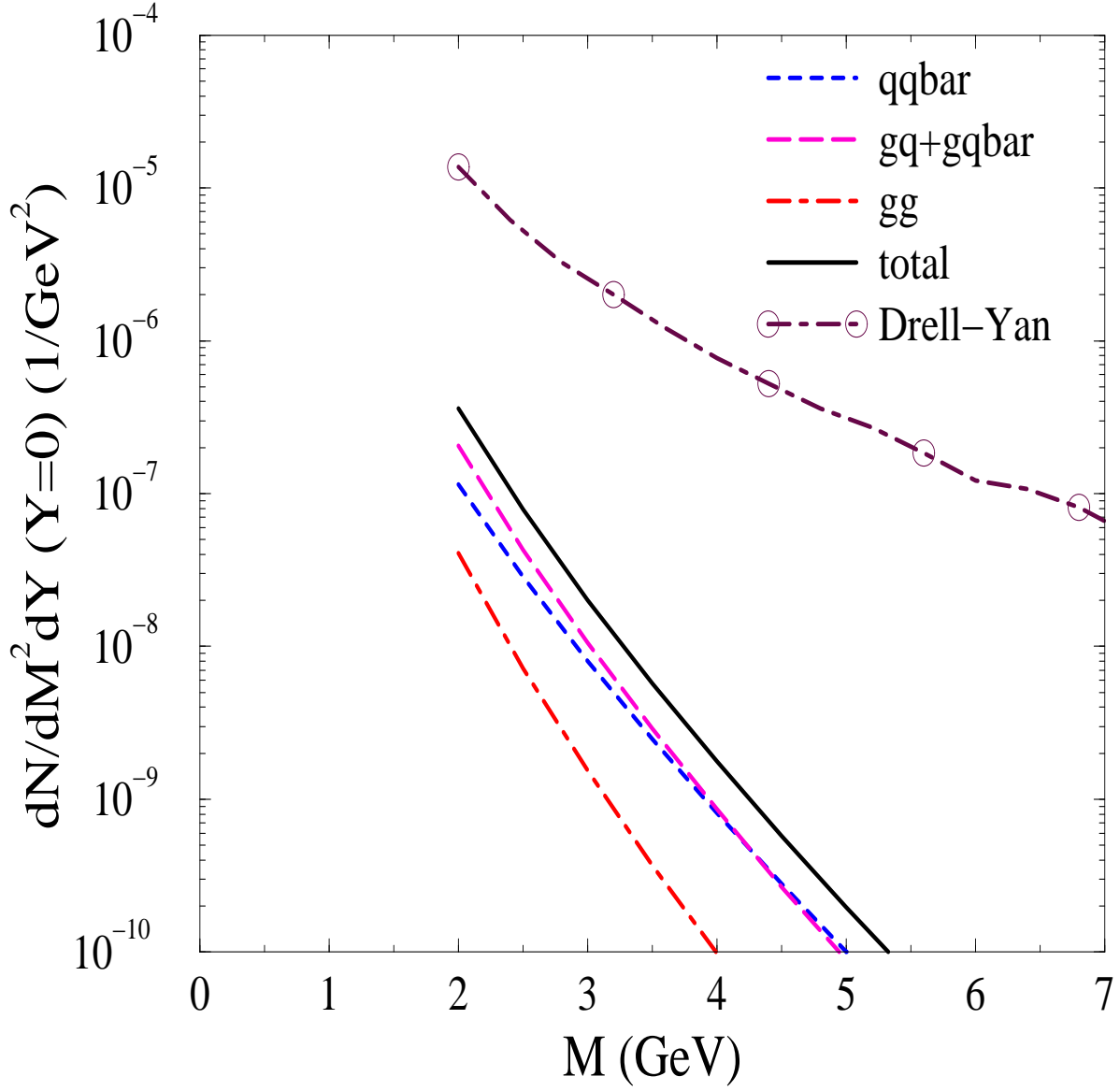


Figure 6: Thermal dilepton yields for central Au+Au collisions at RHIC with initial conditions of $T_0 = 570$ MeV, $\lambda_{g,0} = 0.060$, $\lambda_{q,0} = 0.0072$ and time evolutions according to Eqs.(26) and (28).

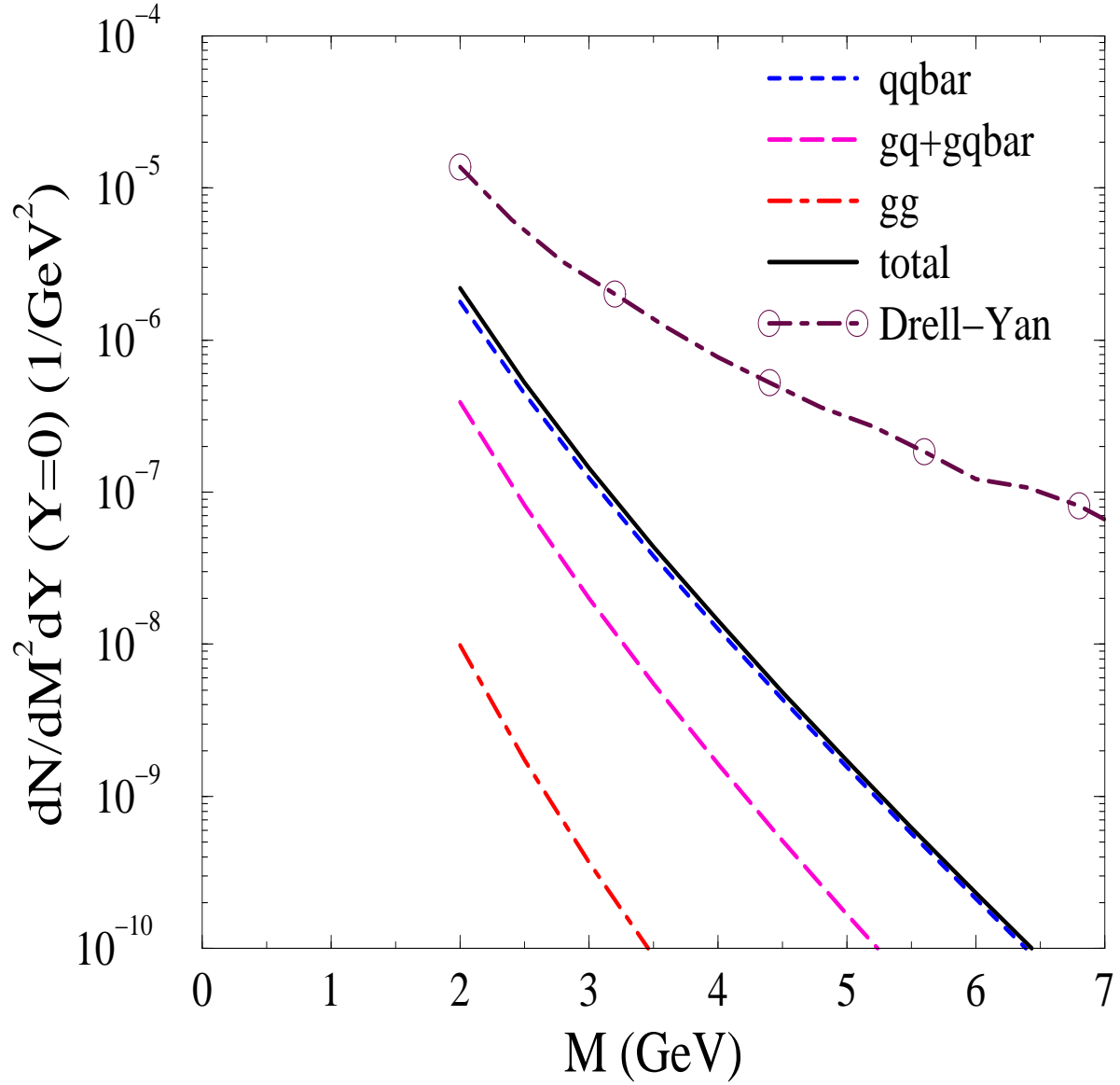


Figure 7: An upper limit of thermal dilepton yields for central Au+Au collisions at RHIC with initial conditions of $T_0 = 570$ MeV and $\lambda_{g,0} = \lambda_{q,0} = 0.028$.

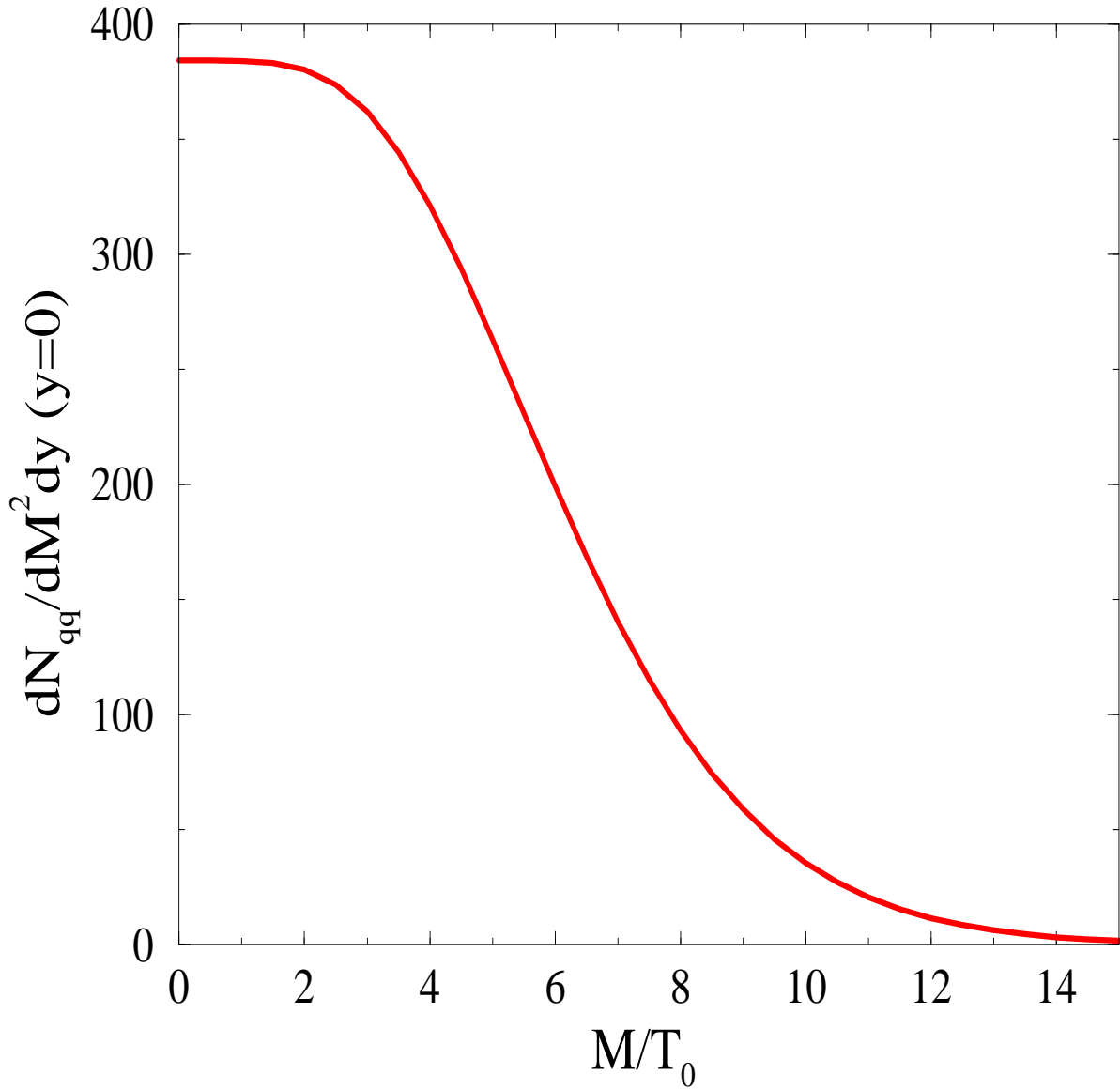


Figure 8: The dependence of the thermal dilepton yield from the LO $q\bar{q}$ annihilation on the initial temperature T_0 with fixed rapidity density of initial transverse energy. See Eq.(36) for the unit of the ordinate.

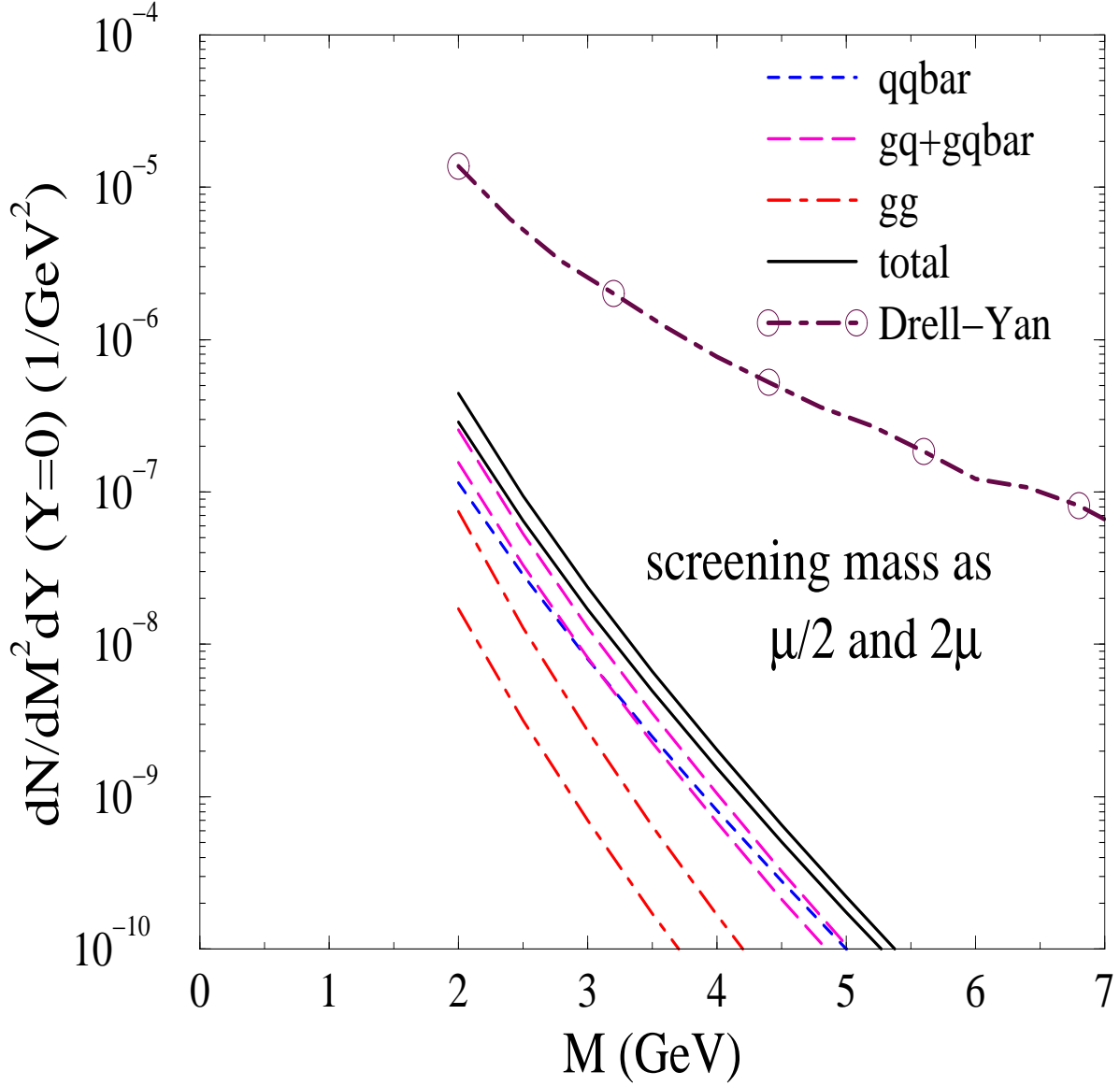


Figure 9: The screening mass dependence of thermal dilepton yields for central Au+Au collisions at RHIC with initial conditions of $T_0 = 570$ MeV, $\lambda_{g,0} = 0.060$ and $\lambda_{q,0} = 0.0072$. The set of upper (lower) curves corresponds to results using half (twice) the thermal quark mass as the screening mass.